

# Device Simulation using Symmetric Smoothed Particle Hydrodynamics

K. Kitayama<sup>1</sup>, M. Toogoshi<sup>2</sup>, and Y. Zempo<sup>2</sup>

<sup>1</sup>Simulatio Corporation, Yokohama 222-0033 Japan

<sup>2</sup>Computer and Information Sciences, Hosei University, Tokyo 184-8584 Japan

E-mail: [zempo@hosei.ac.jp](mailto:zempo@hosei.ac.jp)

**Abstract.** We have applied symmetric smoothed particle hydrodynamics (SSPH) to electronic structure calculations for high electron mobility transistors (HEMTs). In layered structures such as field effect transistors (FETs), and especially HEMTs, the current density is mainly dependent on the electron mobility and the electronic field near the gate, where both can be taken to be constant. The relation between the channel current and the applied gate voltage can be obtained by a one-dimensional calculation. Then, it is easy to apply SSPH to evaluate the simple quantum properties of a device. We mainly focus on the  $I$ - $V$  characteristics, which are typical device features. The electronic structure of a HEMT was calculated using both SSPH and finite-difference (FD) methods. The results from SSPH calculations are in good agreement with those from the FD method, and the accuracy of SSPH is similar to that of FD. In a simple example, where three particles are employed in the SSPH domain, we show there is an equivalence to the three-point method in FD.

## 1. Introduction

Smoothed Particle Hydrodynamics (SPH) is a typical mesh-free particle method, in which the system is represented by a finite set of arbitrarily distributed particles without using any mesh. SPH is widely applied to hydrodynamic problems that deal with complex shapes, large deformations and free surfaces. Recently, SPH-based methods have been applied to solve non-hydrodynamic partial differential equations such as the wave equation, the diffusion equation, Maxwell's equations and Poisson's equation [1, 2, 3, 4]. However, there are few studies for electronic structure calculations [5, 6].

An SPH-based method may lead to an efficient real-space technique because of arbitrarily distributed computation points. However, it is generally known that the standard SPH method has low accuracy [7]. In considering applications of mesh-free particle methods to practical electronic structure calculations, obtaining comparable accuracy to the results of finite-difference (FD) methods is one of the problems. Symmetric Smoothed Particle Hydrodynamics (SSPH) [8, 9] have been proposed as one of the improved techniques. This method successfully increases the accuracy of standard SPH by using a Taylor-series expansion.

We applied SSPH to a practical electronic device calculation for a high-electron-mobility transistor (HEMT). As field-effect transistors (FETs) incorporating heterojunctions, HEMTs have attracted attention due to features such as high gain, high switching speeds and extremely low noise values. These features are suitable for applications in industry such as high-frequency devices and low noise amplifiers [10]. In such a device, a very high current can be provided by

the accumulated electrons, which can be considered as a two-dimensional electron gas (2DEG) [11]. For such a case, calculations of the electronic structure can be expressed using one-dimensional equations. This provides quite a nice example to use in checking the accuracy of SSPH calculations. Non-uniform distributions of computational points can be treated in the frame-work of SSPH, which we expect to reduce computational costs significantly. However, the SSPH calculation described in this paper was performed for a uniform particle distribution for simplicity.

The purpose of this paper is to evaluate SSPH for the simple quantum device of a HEMT. We mainly focus on the  $I$ - $V$  characteristics, which is one of the typical device features. The paper is organized as follows. First, the HEMT structure we adopted is explained, and the formulation of SSPH follows in the next section. The numerical results are shown in Sec. 3. Finally, we summarize the conclusions in the last section.

## 2. Method

A typical, single-heterojunction HEMT is shown in Fig. 1. Usually such a device is fabricated as an epitaxial multi-layer structure. Using the band offset at the heterojunction, electronic devices such as FETs, and especially HEMTs, work quite efficiently. Such devices have been intensively studied both experimentally and theoretically [11, 12]. The electronic charge distribution in this system can be considered as a quasi-2D system. The electric current from the source to the drain is controlled by changing the voltage applied to the gate, which changes the electrostatic potentials around the gate. The current density of the heterostructure FET is determined by the ionized impurities, the gate electric field, and the density and the electron mobility. The electric field is approximately constant in the narrow region beneath the gate. Also, the electron mobility can be taken as constant in the long gate device. Then the current is proportional to the electron density. Thus, in a one-dimensional analysis, in a direction perpendicular to the surface that corresponds to the gate, it is possible to determine the device characteristics, e.g., the relation between the channel current and the applied gate voltage for a practical FET device [10]. The channel is narrow enough to be expressed in terms of quantized states, which are simply described in a one-dimensional (1D) equation.

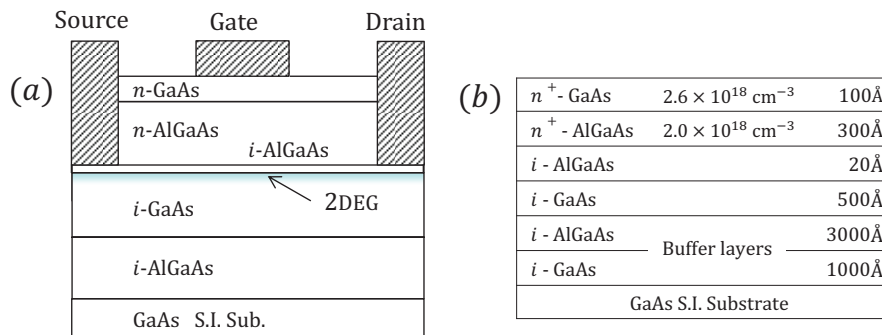


**Figure 1.** The structure of a HEMT. (a) The schematic device model, and (b) the layer structure we adopted in the calculation.

In our general analysis of the characteristic behavior of the device, we solved the effective one-dimensional, one-electron Schrödinger equation and Poisson's equation [15]. In the vertical direction beneath the gate, these equations can be written in 1D as follows;

$$-\frac{\hbar^2}{2} \frac{d}{dz} \left( \frac{1}{m^*(z)} \frac{d\psi_i(z)}{dz} \right) + V(z)\psi_i(z) = E_i\psi_i(z) \quad (1)$$

$$\frac{d}{dz} \left( \varepsilon(z) \frac{d\phi(z)}{dz} \right) = -(\rho_I + \rho_q), \quad (2)$$

where  $E_i$  is the  $i$ -th energy eigenvalue, and  $\psi_i(z)$  is the corresponding wave function. The position-dependent effective mass and permittivity are expressed as  $m^*(z)$ , and  $\varepsilon(z)$ , respectively. The effective potential  $V(z)$  can be obtained from Poisson's equation. The electrostatic potential  $V_H$  can be expressed by  $V_H = -e\phi + \Delta v$ , where  $\Delta v$  is the band offset of the two heterojunction interfaces in the HEMT structure. The potential profile  $\phi$  is determined by the ionized charge  $\rho_I$ .

$$\rho_I = e [p(\phi) + N_D^+(\phi) - N_A^-(\phi) - n(\phi)], \quad (3)$$

and the carrier concentration  $\rho_q(z)$ , which exists mainly in the channel region, is given by

$$\rho_q(z) = \frac{e m^*(z) kT}{\pi \hbar^2} \sum_i g_i |\psi_i(z)|^2 \ln \left[ 1 + \exp \left( \frac{E_F - E_i}{kT} \right) \right]. \quad (4)$$

Here  $g_i$  is the degeneracy of the state,  $E_F$  is the Fermi level,  $T$  is the temperature, and  $k$  is Boltzmann's constant. The electrostatic potential distribution is obtained from a self-consistent solution of the Schrödinger and Poisson equations. Usually, Eqs. (1) and (2) are expressed in finite-difference (FD) form, and are solved subject to appropriate boundary conditions. In addition, matching conditions at the heterojunction interfaces are required for the derivatives of wave functions and electrostatic potentials. The solution can be obtained by solving each equation step-by-step until convergence is achieved [13, 14, 15, 16]. The electronic charge density determines the potential  $V$ , which can also include the exchange-correlation potential.

In SPH, on the other hand, the wave function is approximated using an integral form, and the system is represented by a finite number of particles. The concept of the integral representation of a wave function  $\psi(r)$  starts from the following identity. The delta function is replaced by a kernel function  $W(r, h)$ .

$$\psi(z) = \int_{\Omega} \psi(z') \delta(z - z') dz' \simeq \int_{\Omega} \psi(z') W(z - z', h) dz', \quad (5)$$

where  $h$  is the smoothing length that defines the domain  $\Omega$ . We adopt the Wendland function as the kernel function in the one-dimensional system we consider [17]. It is finite and is convenient for numerical calculations:

$$W(r, h) = \begin{cases} \frac{3r}{4h} \left( 1 - \frac{1}{2} \frac{r}{h} \right)^5 \left\{ 2 \left( \frac{r}{h} \right)^2 + \frac{5r}{2h} + 1 \right\} & (0 \leq \frac{r}{h} \leq 2) \\ 0 & (2 \leq \frac{r}{h}) \end{cases} \quad (6)$$

where  $r = |z - z'|$ .

SSPH corrects the approximation of SPH using a Taylor-series expansion of  $\psi(\mathbf{r})$ . The right-hand side of Eq. (5) can then be rewritten as follows:

$$\int_{\Omega} (z - z_i)^k \psi(z) W(z - z_i, h) dz \simeq \sum_{l=0}^m \left( \int_{\Omega} (z - z_i)^{k+l} W(z - z_i, h) dz \right) \left( \frac{1}{l!} \frac{\partial^l \psi}{\partial z^l} \right) \bigg|_{z_i}, \quad (7)$$

where  $k = 0, 1, \dots, m$ . The integral equation is thus approximated by the summation over the particles in the domain  $\Omega$  corresponding to the smoothing length  $h$ . In this version of SSPH, there is no derivative of the kernel function, which sometimes causes errors in SPH calculations. The accuracy of SSPH mainly depends on the order of the Taylor-series expansion [5]. Equation (7) has the form of simultaneous linear equation,  $P = KD$ , as given below:

$$\begin{aligned} P &= (P_k), & P_k &= \sum_j^N (z_j - z_i)^k \psi(z_j) W_{ij} \Delta V_j \\ K &= (K_{kl}), & K_{kl} &= \int_{\Omega} (z - z_i)^k (z - z_i)^l W(z - z_i, h) dz \\ D &= (D_l), & D_l &= \left( \frac{1}{l!} \frac{\partial^l \psi}{\partial z^l} \right) \bigg|_{z_i}, \end{aligned} \quad (8)$$

where  $W_{ij} = W(z_j - z_i, h)$ . Naturally, the Schrödinger equation in Eq. (1) is a generalized eigenvalue problem. The small volumes occupied by the  $j$ -th particles surrounding particle  $i$  are defined as  $\Delta V_j$ , which is calculated the number density  $n(z_j)$ :

$$\Delta V_j = 1/n(z_j), \quad n(z_j) = \sum_k^m \delta(z_j - z_k) \simeq \sum_k^m W(z_j - z_k; h). \quad (9)$$

Defining  $D_0 = \psi|_{z_i}$ ,  $D_1 = \frac{\partial \psi}{\partial z}|_{z_i}$ , and  $D_2 = \frac{1}{2} \frac{\partial^2 \psi}{\partial z^2}|_{z_i}$ , we can write the Schrödinger and Poisson equations Eqs. (1) and (2) at the position of the  $i$ -th particle in the form of the SSPH discretization. For example, in the simplest case of a constant effective mass, the Schrödinger equation, Eq. (1), for the  $i$ -th particle in SSPH can be written as

$$\begin{pmatrix} V(z_i) & 0 & -\frac{\hbar^2}{m^*} & \dots & 0 \end{pmatrix} D = (E \quad 0 \quad 0 \quad \dots \quad 0) D. \quad (10)$$

Poisson's equation in Eq. (2), with constant permittivity, also can be simply described in a manner similar to the derivation of Eq. (10). From the electronic charge density, the electrostatic potential and the exchange-correlation potentials are also determined. In SSPH, the particle position can be arbitrarily distributed so as to obtain a specified level of accuracy. This is a particular feature of this method, which we expect to reduce the computational cost significantly. However, we have to calculate  $K^{-1}$  in each particle position, keeping the matrix  $K$  regular.

### 3. Results and discussion

We have calculated device characteristics both in SSPH and FD, and have compared the results. In the SSPH calculation, we adopted the smoothing length  $h = 0.2 \text{ \AA}$  and assumed constant particle distributions over the distance  $\Delta x = 0.2 \text{ \AA}$ . For the FD mesh size, we used the same value  $\Delta x = 0.2 \text{ \AA}$  as for the particle distribution in SSPH. Figure 2 shows that band structure and the charge profile of the results from both the SSPH and FD calculations, plotted in the vertical direction. Both results from SSPH are in good agreement with those from the FD calculation.

As mentioned above, the current is determined by the carrier density. The sheet carrier density  $N_s$  and  $dN_s/dV_g$  are plotted in Fig. 3 as functions of the gate voltage  $V_g$ . These provide the  $I$ - $V$  characteristics and the transconductance  $g_m$ , respectively. Changing the applied gate voltage corresponds to calculating the characteristics using different boundary conditions at the

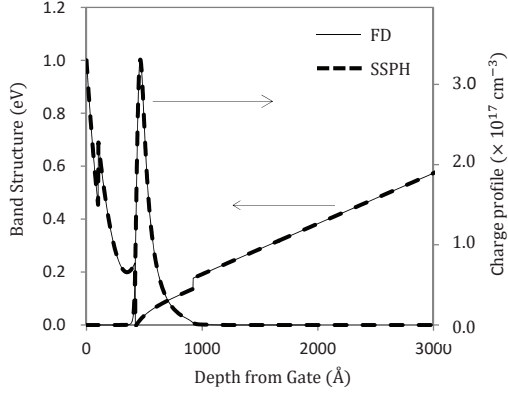


**Figure 2.** Conduction band structure and charge profile, calculated using SSPH (dashed line) and FD (solid line).

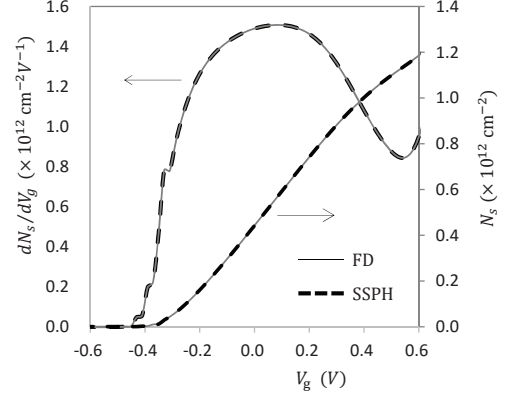


**Figure 3.** Characteristic properties and sheet carrier density  $N_s$  and  $dN_s/dV_g$ , calculated using SSPH (dashed line) and FD (solid line).

surface  $z = 0$ . We have calculated the charge profile for different gate voltages in the steps of  $\Delta V_g = 0.005$ . The sheet carrier density  $N_s$  integrated over the whole region and is plotted in Fig. 3. At each point, we also calculate  $dN_s/dV_g$  using  $\Delta V_g$  in a difference scheme; this is also plotted in Fig. 3. We can see that the results of SSPH are in good agreement with those of FD. The accuracy is sufficient for practical device simulations. In the SSPH calculation, we have also tried the different smoothing length  $h = 0.3$  Å, which includes five particles in the calculation domain, rather than three. The results were the same as for the calculation performed with the smoothing length  $h = 0.2$  Å. Within this difference, the accuracy of SSPH does not change.

There is a significant difference in the form of the SSPH and FD equations. The former is based on integral equations, and the latter on differential equations. However, there is an equivalence in the simplest case, in which SSPH uses three particles in the computational domain, and FD uses a three-point method. The reason is that, from the discretization point of view, there is no difference between SSPH and FD in this case. Let us consider a typical case, as

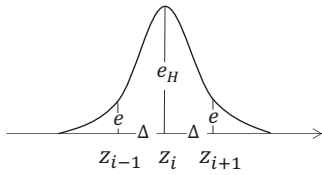


**Figure 4.** Example of the kernel function  $W$  in the case of a constant distribution  $\Delta$  of three particles over the smoothing length. The values at each point are  $W(z_i) = e_H$ , and  $W(z_{i-1}) = W(z_{i+1}) = e$ , respectively.

shown in Fig. 4. Three particles are distributed over a constant spacing  $\Delta$  in the computational domain defined by the smoothing length  $h$ . In this case, the matrix size of  $K$  reduces to  $3 \times 3$ . The inverse matrix  $K^{-1}$  can be calculated manually, and the equation  $D = K^{-1}P$  can then be

expressed as

$$\begin{pmatrix} \psi|_i \\ \frac{\partial}{\partial x}\psi|_i \\ \frac{1}{2}\frac{\partial^2}{\partial x^2}\psi|_i \end{pmatrix} = \begin{pmatrix} \frac{1}{1-2e} & 0 & \frac{1}{(1-2e)\Delta^2} \\ 0 & \frac{1}{2e\Delta^2} & 0 \\ \frac{1}{(1-2e)\Delta^2} & 0 & \frac{1}{2e(1-2e)\Delta^4} \end{pmatrix} \begin{pmatrix} e\psi_{i-1} + e_H\psi_i + e\psi_{i+1} \\ e\Delta(-\psi_{i-1} + \psi_{i+1}) \\ e\Delta^2(\psi_{i-1} + \psi_{i+1}) \end{pmatrix}. \quad (11)$$

We can immediately see the equivalence by substituting each element – that is,  $D_0 = \psi_i$ ,  $D_1 = (-\psi_{i-1} + \psi_{i+1})/(2\Delta)$ , and  $D_2 = (\psi_{i-1} - 2\psi_i + \psi_{i+1})/(2\Delta^2)$  – into Eq. (10). The practical formula obtained from three-point FD can thus be reproduced through the SSPH procedure.

#### 4. Summary

We introduced SSPH as a discretization technique for device simulations. SSPH was applied to an electronic structure calculations for a HEMT. In comparing the characteristics of HEMTs calculated using SSPH and FD, we find that the results from SSPH are in good agreement with those obtained using FD. The accuracy of SSPH is similar to that of FD. From the technical point of view, the computational effort increases as the order of the Taylor-series expansion becomes higher. However, SSPH and FD were also shown to be equivalent in a simple case corresponding to the three particles in the SSPH computational domain and to a three-point FD method. If the number of SSPH particles is large enough to describe steep changes in the one-dimensional Schrödinger equation, reasonable accuracy can be obtained. Our results indicate that SSPH can be applied to other electronic-structure calculations that require high accuracy.

#### Acknowledgments

The authors would like to express their gratitude to Professor S. S. Kano for useful discussions and encouragement. This work was partially supported by JSPS Grants-in-Aid for Scientific Research (C) Grant number 16K05047, Sumitomo Chemical Co., Ltd. and Simulation Corporation. Computations were partially performed at the Research Institute for Information Technology, Kyushu University and the Supercomputer Center.

#### References

- [1] Laguana P 1995 *Astrophys. J.* **439**, 89
- [2] Stranex T and Wheaton S 2011 *Comput. Method. Appl. Math.* **B200**, 392
- [3] Tascano E, Balasi G D and Tortorici A 2012 *Appl. Math. Comput.* **218**, 8906
- [4] Ala G, Francomano E, Tortorici A, Tascano E and Viola F 2006 *J. Comput. Appl. Math.* **191**, 194
- [5] Sugimoto S and Zempo Y 2014 *J. Phys.: Conf. Ser.* **510**, 012037
- [6] Zempo Y and Sugimoto S 2015 *J. Phys.: Conf. Ser.* **640**, 012031
- [7] Lucy L B 1977 *Astron. J.* **439**, 1013
- [8] Batra R C and Zhang G M 2008 *Compt. Mech.* **41**, 527
- [9] Zhang G M and Batra R C 2009 *Compt. Mech.* **43**, 321
- [10] Hata M, Fukuhara N, Sasajima Y, and Zempo Y, 2000 *Sumitomo Kagaku* **2000-I**, 10
- [11] e.g. Sze M, 1981 *Physics of Semiconductor Devices*, 2nd ed. (Wiley, New York)
- [12] Adachi S, et. al. 1982 *Rev. Mod. Phys.* **54**, 437 (Wiley, New York, ).
- [13] Stern F, 1972 *Phys. Rev.* **B5**, 4891
- [14] Venter B, 1978 *Sol. Stat. Comm.* **28**, 861
- [15] Stern F and Sarma S, 1984 *Phys. Rev.* **B30**, 840
- [16] Tan I.-H, Snider G L Chang L D Hu E L, 1990 *Appl. Phys.* **68**, 4071
- [17] Wendland H 1995 *Adv. Comput. Math.* **4**, 389